

Accurate Analytical Solution for Free Vibration of the Simply Supported Triangular Plate

Daniel J. Gorman*

University of Ottawa, Ottawa, Ontario, Canada

Exploiting the superposition method developed earlier by the author, a highly accurate analytical-type solution is obtained for the free vibration of the general simply supported triangular plate. A new technique is introduced for the orderly storage of eigenvalues. It is shown how advantage can be taken of the more easily obtained isosceles triangular plate solutions. Accurate eigenvalues are tabulated for a wide range of plate geometries. This represents the first accurate and comprehensive treatment of this problem to appear in the literature.

Nomenclature

- a = length of base of right triangle
 b = length of vertical edge of right triangle
 D = plate flexural rigidity, $= Eh^3/[12(1 - \nu^2)]$
 E = Young's modulus of plate material
 h = plate thickness
 K = upper limit in series expansions
 K^* = upper limit in first summation of series expansions
 M = amplitude of applied bending moment
 W = plate lateral displacement
 ξ = distance along plate edge divided by a
 η = distance along plate edge divided by b
 λ^2 = $\omega a^2 \sqrt{\rho/D}$
 λ^{*2} = $\omega b^2 \sqrt{\rho/D}$
 ω = circular frequency of plate vibration
 ρ = mass of plate per unit area
 ϕ = plate aspect ratio b/a
 ϕ' = inverse of plate aspect ratio a/b

Introduction

It is well known that there is a serious lack of information available in the literature concerning the free vibration frequencies and mode shapes of triangular plates. Most of the results are approximate in nature and only a limited number of geometries and mode shapes are treated. This discrepancy in the literature is, of course, due to the formidable problem of trying to find solutions that satisfy both the governing differential equation and the prescribed boundary conditions.

In this paper, a new approach toward the free vibration analysis of triangular plates is undertaken and an accurate analytical-type solution is developed for the general triangular plate with simple support along the edges. A new technique is proposed for the storage of eigenvalues and frequency and mode shape information is provided in an orderly manner for a wide range of plate geometries and free vibration mode shapes. The analysis is performed by means of the superposition technique that has already been exploited by the author in obtaining solutions to numerous plate vibration problems.

Proposed Eigenvalue Storage Map

In the author's opinion, the methods advanced thus far in the literature for the storage and presentation of eigenvalues of triangular plates are unsatisfactory.¹ Accordingly, a new scheme, or storage map, is presented here. Reference is made to the storage map as depicted in Fig. 1. Initially, we consider only triangular plates with simple support on all edges.

Let the heavy line running along the base of Fig. 1 represent the longest edge, or base, of the triangular plate of interest. It is agreed, then, that any possible triangle whose upper apex (the joining of the two shorter edges) lies to the right of the centerline of the figure must lie in the area enclosed by this center line and the circular arc of the right-hand side of the figure. In fact, due to symmetry, we need consider only those triangles whose upper apex lies on the boundaries of this region or within it.

We next observe that all triangles whose apex lies on the boundaries of this region will in fact be isosceles triangles (two edges of equal length). This is an important observation since, as will be seen later, the family of isosceles triangles are much more easily analyzed than the general triangle.

The remaining possible triangles must, of course, have their apex within the region as discussed above. In order to proceed in an orderly fashion, a rectangular grid of points has been laid out within this region. Eigenvalues are stored for each of these points. It will be appreciated that designers who use this grid will have to interpolate for plates whose apex does not lie on one of the grid points. The grid has been chosen with a view toward minimizing the amount of interpolating needed and thereby improving accuracy. It will be noted that distances measured along the axes of the figure are nondimensionalized with respect to the base length of the triangle.

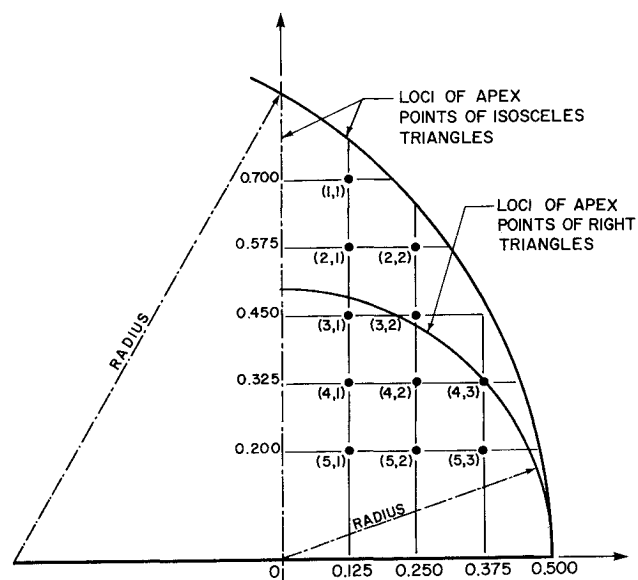


Fig. 1 Eigenvalue storage map for general simply supported triangular plate (longest edge of triangle lies along base; solid dots represent upper apex of triangles for which eigenvalues are stored; distances are nondimensionalized with respect to base).

Received Aug. 26, 1987; revision received March 10, 1988. Copyright © 1989 by D. J. Gorman. Published by the American Institute of Aeronautics and Astronautics, Inc., with permission.

*Professor, Department of Mechanical Engineering.

Analytical Procedure

Analysis of Isosceles Triangles

Let us consider an isosceles triangle with simple support along all edges as shown in Fig. 2. It will be appreciated that all free vibration modes of this plate will either be of the symmetric type, i.e., modes that are symmetric about the central vertical axis of the plate or modes that are antisymmetric, i.e., antisymmetric with respect to this same axis. It is seen that analysis of the antisymmetric modes is accomplished if one analyzes the right half of the triangle only, i.e., a right triangle with simple support along all edges. Such an analysis has already been performed by the author and is described in detail in Ref. 2. The reader should study this earlier report as it contains a basic description of the superposition technique exploited here. These details will not be repeated in this paper.

We turn next to the analysis of the symmetric modes of the isosceles triangle. The procedure followed is similar to that of Ref. 2 except that different building blocks are employed and advantage is taken of some recent advances in application of the superposition method.³ We begin by focusing our attention on the four rectangular plate forced vibration solutions, or building blocks, of Fig. 3.

Each building block has simple support along its upper edge and slip shear conditions along the left-hand edge. These latter conditions, indicated by two small adjacent circles, require that there should be no slope taken normal to the edge and that there should be no vertical edge reaction. The first building block has simple support conditions imposed along its right-hand edge and a condition of zero displacement imposed along its driven edge. This edge is driven by a distributed harmonic bending moment of circular frequency ω with distributed amplitude given by

$$M(\xi) = \sum_{m=1,3,5}^{\infty} E_m \cos \frac{m\pi\xi}{2} \quad (1)$$

The solution for this plate response is taken in the form

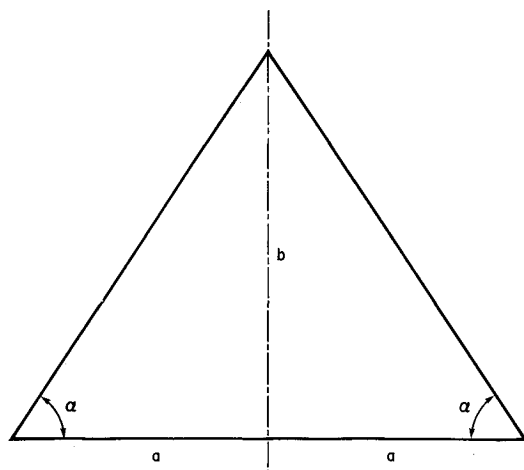


Fig. 2 Simply supported isosceles triangle.

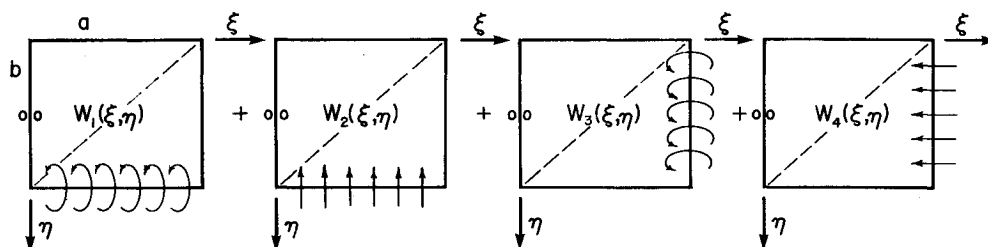


Fig. 3 Building blocks used in analyzing the isosceles triangle symmetric modes.

proposed by Lévy⁴ as,

$$W(\xi, \eta) = \sum_{m=1,3,5}^{\infty} Y_m(\eta) \cos \frac{m\pi\xi}{2} \quad (2)$$

Following the steps as outlined in Ref. 2, it is readily shown that the solution for Eq. (2) is given by

$$W_1(\xi, \eta) = \sum_{m=1,3,5}^{K^*} E_m \left(\theta_{11m} \frac{\sinh \beta_m \eta}{\sinh \beta_m} + \theta_{13m} \frac{\sin \gamma_m \eta}{\sin \gamma_m} \right) \cos \frac{m\pi\xi}{2} \\ + \sum_{m=K^*+2}^{\infty} E_m \left(\theta_{22m} \frac{\sinh \beta_m \eta}{\sinh \beta_m} + \theta_{23m} \frac{\sinh \gamma_m \eta}{\sinh \gamma_m} \right) \cos \frac{m\pi\xi}{2} \quad (3)$$

where $\beta_m = \phi \sqrt{\lambda^2 + (m\pi/2)^2}$, $\gamma_m = \phi \sqrt{\lambda^2 - (m\pi/2)^2}$ or $\phi \sqrt{(m\pi/2)^2 - \lambda^2}$, whichever is real, and the first summation contains only those terms for which $\lambda^2 \geq (m\pi/2)^2$. Furthermore, we have

$$\theta_{11m} = -1/(\beta_m^2 + \gamma_m^2)$$

$$\theta_{13m} = -\theta_{11m}, \theta_{22m} = -1/(\beta_m - \gamma_m^2)$$

$$\theta_{23m} = -\theta_{22m}$$

Boundary conditions for the nondriven edges of the second building block of Fig. 3 are identical to those of the first. Along the driven edge, a condition of zero bending moment is imposed and the edge is driven by a distributed harmonic displacement of circular frequency ω . The distribution of the amplitude of this displacement is again represented by a series identical to that of Eq. (1). The solution $W_2(\xi, \eta)$ will have a form identical to that of Eq. 3. The quantities θ_{11m} , θ_{13m} , etc., will involve different expressions, however. These may be designated as ϕ_{11m} , ϕ_{13m} , etc., in order to avoid confusion.

Solutions for the remaining two building blocks of Fig. 3 are readily obtained following the procedures described above and in Ref. 2. In each case, a condition of simple support is imposed along the lower edges ($\eta = 1$). The Lévy-type solutions must, therefore, involve the sine functions and they can be written in the form

$$W(\xi, \eta) = \sum_{m=1,2}^{\infty} Y_m(\xi) \sin m\pi\eta \quad (4)$$

The third building block has a condition of zero displacement imposed along its driven edge. This edge is driven by a harmonic bending moment similar to that described for the first building block. Amplitude of this moment is expanded in series form as

$$M(\eta) = \sum_{m=1,2}^{\infty} E_m \sin m\pi\eta \quad (5)$$

The fourth building block has a condition of zero bending moment imposed along its driven edge. This edge is driven by an imposed harmonic displacement as described for the second building block. Amplitude of this displacement is expanded in series form of the type utilized in Eq. (5). The solution for Eq. (4), unlike that provided in Eq. (2), will

involve the hyperbolic cosine functions and the trigonometric cosine functions. This is because slip shear conditions instead of simple support conditions must be imposed along the edge opposite the driven edge.

Determination of the eigenvalues and mode shapes for this family of triangles is achieved following the general procedure of Ref. 2, but taking advantage of modifications as introduced later in Ref. 3. The procedure to be followed is outlined here, briefly, for the interested reader.

We begin by superimposing the four building blocks of Fig. 3, one on top of the other, to form a single rectangular plate composed of the four solutions. Since each solution satisfies the governing differential equation exactly, the combined solution will also exactly satisfy this equation. We focus our attention on the right triangular portion of the plate lying above the broken diagonals shown in Fig. 3. It is noted that the edges of this triangular portion, $\xi = 0$ and $\eta = 0$, satisfy the desired slip shear and simply supported conditions, respectively.

We next wish to satisfy the condition of zero lateral displacement and bending moment along the hypotenuse of the triangular region. We vary the trial eigenvalues λ^2 with a view to finding that value which will permit a nontrivial solution for the driven edge coefficients discussed above and satisfaction of the simple support conditions along the broken-line diagonal of the plate. This value of λ^2 will be the sought-after eigenvalue.

Letting the number of driving coefficients in each building block equal K , we obtain $4K$ contributions to displacement along the diagonal. These contributions are expanded in a Fourier series along the diagonal of $2K$ terms. Setting the net coefficient of each Fourier term equal to zero gives rise to $2K$ linear homogenous algebraic equations involving the driving coefficients. Further $2K$ equations are obtained upon expanding the contributions to the moment along the diagonal in the same fashion.

We therefore have $4K$ equations involving the $4K$ unknown driving coefficients. The final step is to vary the trial value of λ^2 until we obtain that value which causes the determinant of the coefficient matrix for this system of equations to vanish. This value of λ^2 is, of course, the eigenvalue. We may then proceed to seek the higher eigenvalues, as desired. In effect, the above driving coefficients are constrained so as to induce simple support edge conditions along the diagonal. The value of K may be augmented in order to check convergence. With the eigenvalue established, one of the driving coefficients may be set equal to unity and the resulting set of nonhomogenous

equations solved to obtain the remaining coefficients. The mode shape associated with the eigenvalue can then be plotted.

Analysis of the General Triangle

This analysis is conducted by means of the building blocks of Fig. 3 coupled with those of Fig. 5. Let us consider a simply supported triangle whose upper apex falls on the point (1,1) of Fig. 1, for example. It is seen that this triangle, like all such triangles, is composed of two right triangles whose common boundary lies along the vertical line joining the apex of this main triangle to the base (Fig. 4). Each right triangle will have its own aspect ratio (ratio of height to base length).

The solution for this general triangular plate problem is achieved in a manner differing only slightly from that described above for the isosceles triangle. One begins by obtaining solutions for the building blocks of Fig. 5. Each building block has simple support along its upper edge with slip shear conditions along its lower edge. Solutions will, therefore, be taken in the form expressed by Eq. (2) with ξ and η interchanged and the cosine functions replaced by sine functions. The first building block in the figure has slip shear conditions imposed along its right-hand edge. While it is a matter of choice, the author prefers to first solve this problem with the driven and nondriven conditions along the vertical edges interchanged and then replace the variable ξ by the quantity $1 - \xi$. Before interchange of the variable, the building block will be similar to the third building block of Fig. 3.

The second building block of Fig. 5 differs from the first in that a condition of zero slope taken normal to the boundary is enforced along the driven edge. This condition is represented in the figure by two heavy dots joined by a short line. A distributed harmonic edge displacement is enforced along this edge.

With the above solutions available, and utilizing the aspect ratio of the right triangle to the right-hand side in Fig. 4, one can write a system of equations involving the unknown driving coefficients, which requires that displacement and moment should vanish along the hypotenuse of the associated right triangle. One also has available a set of equations for expressing the displacement, slope, etc., along the vertical edge of the same triangle.

The next step is to repeat the computations, this time using the aspect ratio of the right triangle to the left-hand side in Fig. 4. Again, we require the vanishing of moment and displacement along the diagonal of the right triangle. This time, however, an additional set of equations can be written. We enforce the continuity of displacement, slope, bending moment, and vertical edge reaction along the common boundary of the two right triangular plates (Fig. 4). This gives us exactly the number of equations required to set up the eigenvalue matrix. Determination of eigenvalues and mode shapes then proceeds in the usual manner.

It should be pointed out that preparation of a computer code for analyzing the general, simply-supported, triangular plate problem is less complicated than might at first appear to be the case. The same code used to generate that portion of the eigenvalue matrix associated with the first right triangle above is also utilized to generate the portion associated with the second. It is necessary only to change the aspect ratio and repeat the computation.

Eigenvalue Computation

Isosceles Triangle Symmetric Modes

In view of the difficulty of finding reliable published data with which to make comparison, it is necessary to take all reasonable steps to assure that computed eigenvalues are correct. It is known that exact eigenvalues for simply supported right triangular plates with aspect ratio equal unity can be inferred from the exact solutions available for square plates.⁵ The same is true for the right triangles analyzed here. Accordingly, in computing eigenvalues for these right triangles, the

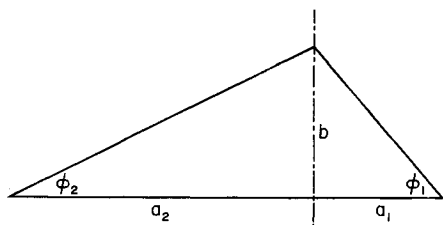


Fig. 4 Combination of right triangles making up the general simply supported triangular plate.

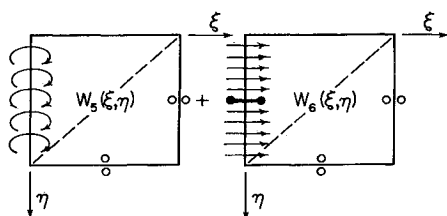


Fig. 5 Building blocks used in conjunction with those of Fig. 3 in analyzing the general simply supported triangular plate (joined solid dots indicate zero slope).

Table 1 Eigenvalues $\lambda^2 = \omega a^2 \sqrt{\rho/D}$ for the first three symmetric vibration modes of the simply supported isosceles triangle ($\phi \geq 1$, $\phi = b/a$)

Mode	1.0	1.25	1.50	1.75	2.0	2.25	2.50	2.75	3.0
1	24.67	18.75	15.28	13.02	11.46	10.31	9.423	8.730	8.178
2	64.15	47.25	36.98	30.31	25.70	22.36	19.86	17.91	16.33
3	83.89	68.47	59.36	52.09	44.33	38.03	33.21	29.47	26.43

Table 2 Eigenvalues, $\lambda^{*2} = \omega b^2 \sqrt{\rho/D}$ for the first three symmetric vibration modes of the simply supported isosceles triangle ($\phi^1 \geq 1$, $\phi^1 = a/b$)

Mode	1.0	1.25	1.50	1.75	2.0	2.25	2.50	2.75	3.0
1	24.67	21.31	19.22	17.81	16.78	16.01	15.41	14.91	14.50
2	64.15	55.02	47.68	42.07	37.84	34.60	32.05	30.01	28.33
3	83.89	69.43	62.33	58.20	55.27	52.71	49.52	45.98	42.83

same procedure was followed as in Ref. 2. All computations were initiated at the known eigenvalues for the case $\phi = 1$ and continuous curves were generated as plots of eigenvalues vs aspect ratio. Because of the formulation of the eigenvalues, these curves decrease monotonically with increase of aspect ratio (or its inverse for $\phi \leq 1$). Following this procedure adds significantly to the confidence that can be placed in the results.

A second point to be considered is the number of terms K to be used in the series solutions. Numerous convergence tests were conducted. It was decided to utilize 14 terms in the final pass when obtaining eigenvalues for this set because experience indicated that, in general, more terms would not lead to changes in the first four significant digits.

General Triangular Plate Problem

The object of these computations was to generate eigenvalues associated with the grid points of Fig. 1. Again, several steps were taken in order to assure accuracy. As a first verification step, an analysis was made of the 60–30 triangle (a right triangle with internal angles of 60 and 30 deg), treating it as a general triangular plate problem. The eigenvalue for this right triangle is known with high accuracy as a result of earlier studies and as inferred by the method of images.² Based on this latter method, it has been found equal to 30.704. It will be appreciated that its upper apex on Fig. 1 will be close to the grid point (3,2). This triangular plate was analyzed, using the general two-right-triangle approach as described above and excellent agreement with the known eigenvalue was obtained.

All computations made in connection with eigenvalues associated with the grid points of Fig. 1 were initiated on the vertical central axis of the figure. The first point selected lay at the intersection of this axis and a horizontal line passing through the grid point of interest. Eigenvalues associated with the starting point were, of course, available from the earlier isosceles triangular plate studies. The first step was to verify that the general triangular plate solution agreed with the previously computed eigenvalues for the corresponding isosceles triangle. Following this, the computational procedure involved moving the apex point of the general triangle in small increments to the right, along the horizontal line, and establishing the eigenvalues at each point. In this way, a continuous trace of the eigenvalues associated with each mode was generated until arrival at the grid point of interest was achieved. Having stored the eigenvalues associated with this point, the procedure was continued until the eigenvalues associated with the last grid point on the horizontal line were obtained. Computations related to another horizontal grid line were then initiated.

A further verification of the general triangular plate computations was carried out in the region of grid point (4,3) of Fig. 1. It will be observed that the loci of apex points of right triangles passes very close to this grid point. In fact, if one continues beyond the grid point in a horizontal direction to the

Table 3 Eigenvalues, $\lambda^2 = \omega a^2 \sqrt{\rho/D}$, for the first three antisymmetric vibration modes of the simply supported isosceles triangle ($\phi = b/a$)

Mode	1.0	1.25	1.50	1.75	2.0	2.25	2.50	2.75	3.0
1	49.35	39.98	34.28	30.48	27.76	25.72	24.08	22.88	21.85
2	98.70	78.78	65.59	56.47	49.88	44.95	41.06	38.09	35.62
3	128.3	105.1	91.86	82.75	74.67	66.98	60.54	55.33	51.08

Table 4 First five eigenvalues, λ^2 for grid points of Fig. 1^a

Coord	1	2	3	4	5
(1,1)	9.325	20.20	23.28	34.42	40.39
(2,1)	11.73	24.14	30.35	40.51	49.44
(2,2)	5.321	10.64	14.15	17.37	23.02
(3,1)	16.05	30.85	42.34	51.59	63.45
(3,2)	7.287	13.67	19.83	22.01	29.62
(4,1)	25.42	44.66	63.03	78.85	89.12
(4,2)	13.14	19.85	28.80	34.45	40.67
(4,3)	2.997	5.014	7.305	8.996	9.985
(5,1)	54.37	84.71	113.5	143.6	117.8
(5,2)	24.60	37.61	50.99	64.31	77.54
(5,3)	6.369	9.514	12.85	16.40	19.80

^a $\lambda^2 = \omega a^2 \sqrt{\rho/D}$, where a equals horizontal distance from grid point to extreme right end of base of general triangle (Fig. 1).

abscissa 0.379967, one intercepts this loci. It is then possible to compare the eigenvalues computed by the general approach with those computed using the single-right-triangle approach. This verification test has been performed for the first four eigenvalues and very good agreement was obtained.

The aspect ratio of the right triangle, i.e., the ratio of the lengths of its perpendicular edges, equals 2.706. The first four eigenvalues for this triangle, nondimensionalized with respect to the shorter of the two perpendicular edges, are 23.08, 38.56, 56.14, and 69.37. It will be noted that they differ only slightly from those given in Ref. 2, with aspect ratio equal 2.75.

Presentation of Computed Results

Isosceles Triangles

Computed eigenvalues for the first three symmetric modes of free vibration of simply supported isosceles triangles are presented in Tables 1 and 2. The data of Table 1 pertain to isosceles triangles whose aspect ratio (ratio of height to half the base) is equal or greater than one. Table 2 compliments Table 1 in that it provides data for triangles with aspect ratios equal to or less than one.

Table 3 presents data for antisymmetric modes of the same triangles. Because of symmetry, it is necessary to consider only cases where the aspect ratio is equal or greater than one. The data of Table 3, which correspond to data published earlier,² has been recomputed here using the modifications discussed in Ref. 3 and is included in the interest of completeness.

General Simply Supported Triangle

The first five eigenvalues computed for each of the internal grid points of Fig. 1 are presented in Table 4. All eigenvalues are nondimensionalized with respect to the base length of the right triangle to the right-hand side of Fig. 1. Suppose we are examining the eigenvalues associated with grid point (2,2), for example. The reference length a on which the eigenvalue is formulated is then equal to (0.50–0.25) times the total base length (longest edge length) of the general triangle. To analyze any simply supported triangle, it is necessary only to establish where its upper apex lies on Fig. 1. Of course, it will be necessary to interpolate if the apex does not lie on a grid point.

Summary and Conclusions

The data provided herein supply the analyst with the first accurate and orderly arranged eigenvalues for the free vibration analysis of simply supported triangular plates. Mode

shape and stress information may also be obtained provided the analyst is prepared to write the building block expressions and generate the eigenvalue matrix. Many such triangles will fall into the category of right or isosceles triangles and, where possible, advantage has been taken of this fact in order to simplify the computation.

The objectives pursued here have been twofold in nature. An orderly description of the theoretical model and the computational procedure have been provided. Of equal importance has been the presentation, for the first time, of a comprehensive listing of accurate eigenvalues for the simply supported triangular plate, regardless of its geometry.

It is true that solutions to problems of the type discussed here may be achieved by less accurate means such as the finite-element methods. Data reported here cannot only serve the designer well but also provide a reference base against which less accurate methods may be compared for verification. It will be appreciated that the analytical method described here is tractable and, unlike numerical methods, the contribution of each component (building block) to the overall solution can be isolated and verified.

It will be appreciated that triangles with combinations of other classical boundary conditions can be analyzed in a simi-

lar manner. It will not always be possible, of course, to exploit all of the simplifications utilized here, particularly if the boundary conditions along each edge are not identical. In some cases it will be necessary to consider grid points on each side of the centerline of Fig. 1.

It is hoped that the technique of eigenvalue computation and storage set forth here will serve as a first step in resolving the problem of free vibration analysis of triangular plates with all combinations of classical edge conditions.

References

- ¹Leissa, A. W., *Vibration of Plates*, NASA SP-160, 1969.
- ²Gorman, D. J., "A Highly Accurate Analytical Solution for Free Vibration Analysis of Simply Supported Right Triangular Plates," *Journal of Sound and Vibration*, Vol. 89, No. 1, July 1983, pp. 107-118.
- ³Gorman, D. J., "A Modified Superposition Method for the Free Vibration Analysis of Right Triangular Plates," *Journal of Sound and Vibration*, Vol. 112, Jan. 1987, pp. 173-176.
- ⁴Timoshenko, S. and Woinowsky-Krieger, S., "Theory of Plates and Shells," 2nd ed., McGraw-Hill, New York, 1959.
- ⁵Gorman, D. J., "Free Vibration Analysis of Rectangular Plates," Elsevier/North-Holland, New York, 1982.

*Recommended Reading from the AIAA
Progress in Astronautics and Aeronautics Series . . .*



Thermophysical Aspects of Re-Entry Flows

Carl D. Scott and James N. Moss, editors

Covers recent progress in the following areas of re-entry research: low-density phenomena at hypersonic flow conditions, high-temperature kinetics and transport properties, aerothermal ground simulation and measurements, and numerical simulations of hypersonic flows. Experimental work is reviewed and computational results of investigations are discussed. The book presents the beginnings of a concerted effort to provide a new, reliable, and comprehensive database for chemical and physical properties of high-temperature, nonequilibrium air. Qualitative and selected quantitative results are presented for flow configurations. A major contribution is the demonstration that upwind differencing methods can accurately predict heat transfer.

TO ORDER: Write AIAA Order Department,
370 L'Enfant Promenade, S.W., Washington, DC 20024

Please include postage and handling fee of \$4.50 with all orders.
California and D.C. residents must add 6% sales tax. All foreign
orders must be prepaid. Please allow 4-6 weeks for delivery.
Prices are subject to change without notice.

1986 626 pp., illus. Hardback
ISBN 0-930403-10-X
AIAA Members \$59.95
Nonmembers \$84.95
Order Number V-103